

PHASE NOISE, COHERENCY, AND CLUTTER SUPPRESSION

James J. Stagliano, Jr.* , James Helvin, James L. Alford, and Dean Nelson
DRS Weather Systems, Inc.

1. INTRODUCTION

Clutter is an unwanted radar return from nonmeteorological targets. Typically, these clutter targets are stationary, hard targets such as building, mountains, towers, etc. Other clutter returns, sea clutter, aircraft, birds, ships, and anomalous propagation are not from stationary products and thus are more difficult to characterize.

Clutter suppression is a feature of modern weather radar. The clutter filter consists of a high pass filter, eliminating the returns with low radial velocity (ideally zero velocity) characteristic of stationary clutter. The clutter filter is typically specified as the type of filter (Finite Impulse Response, FIR, or Infinite Impulse Response, IIR), the delay inherent in the filter (number of poles or points), the rejection depth of the clutter (50 dB), and their width ($0.05f_{PRF}$). Table I summarizes the filter specifications from a number of weather radar signal processors.

Table I The filter specifications from a number of weather radar signal processors.

Signal Processor	Filter Type	Poles	Pub. Depth (dB)	Meas. Depth (dB)
RVP-5	FIR	11	37	37
RVP-6	IIR	4	40	40
ESP-7	IIR	3	50	45
EDRP-8	IIR	4	50	45
EDRP-9	IIR	3	50	65
WSR-88D	IIR	5	50	65

Though not obvious from manufacturer descriptions, the maximum rejection depth of the clutter filter does *not* specify the maximum suppression supported by the system as a whole, rather it denotes a maximum guaranteed rejection if the system will support it. This is emphasized by the last column of Table I which shows measured clutter suppressions for a number of systems.

Another typical performance specification for a weather radar is the phase noise specification. Since a Doppler radar measures the Doppler shift through the phase shift induced by the different frequency, the

phase noise of the system will limit the systems ability to differentiate velocity. As the clutter filters operation depends upon the ability to differentiate velocity (rejects those signals with low velocity), the system phase noise provides a limit to the amount of clutter rejection. This limit is specified by taking the variance of the phase and converting to decibel radians. Mathematically, this is written,

$$CS = -20 \log(\Delta\phi). \quad (1)$$

The phase noise of the system is affected by a great many of the major components of the system. These components include the STABLE Local Oscillator (STALO), modulator, power supply, power oscillator (magnetron) or amplifier (klystron) as well as the myriad of other smaller components. Table II lists the phase noise specification for a number of weather radar systems and the associated maximum clutter suppression.

Table II The phase noise specification for a number of weather radar systems and the associated maximum clutter suppression

Radar System	Max Phase Noise (deg)	Maximum Clutter Rejection (dB)
DWSR2501C	0.5	41
TVDR2500C	0.6	40
DWSR2501C/K	0.1	55
DWSR8501S	0.5	41
DWSR8501S/K	0.1	55
WSR-88D	0.18	50

The maximum clutter suppression that is possible is directly related to the phase noise of the system provided the clutter filters have enough depth and a signal to noise ratio greater than the filter depth.

The signal to noise ratio (SNR) is as defined, the ratio of the signal power to the noise power. This ratio is typically described in logarithmic units (dB). The SNR presents another fundamental limit to the maximum clutter suppression, for the signal cannot be suppressed (or accurately measured if it was) below

* Corresponding Author Address: James J. Stagliano, Jr.,
DRS Weather Systems, Inc.,
128 S. Industrial Blvd., Enterprise, AL 36330;
e-mail: stag@drs-ws.com

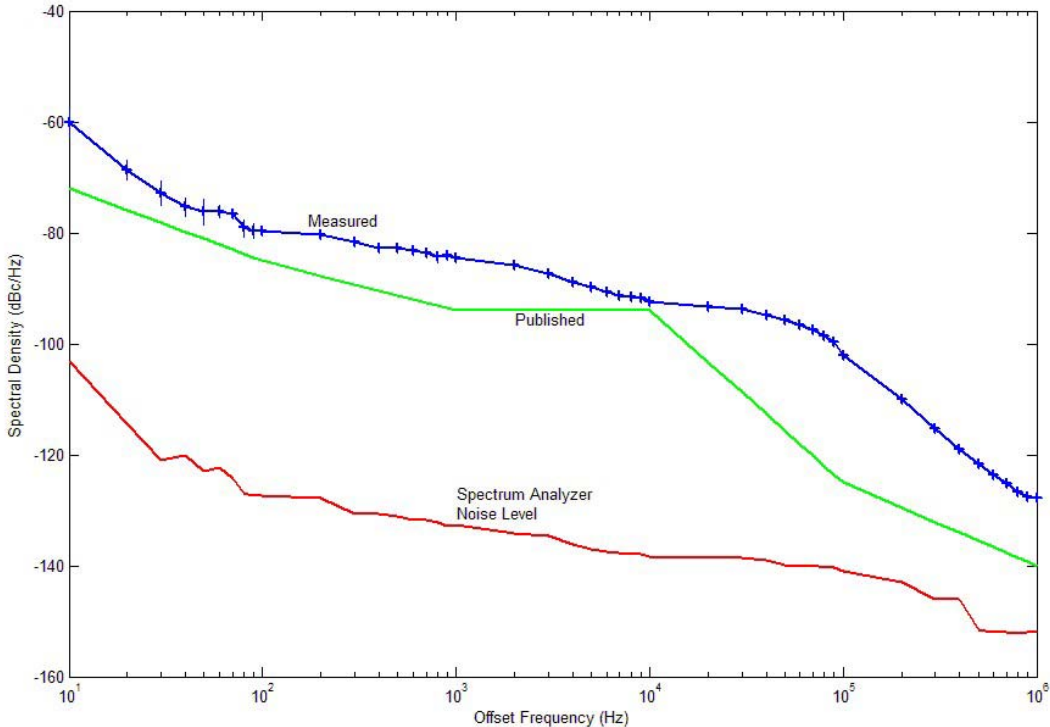


Figure 1. The spectral data in blue plotted along with the manufacturer reported data in green. The red curve is the noise floor of the measurement system. The manufacturer provided data in green is shows less noise than the measured results..

the noise level. In fact, another definition of phase noise is the reciprocal of the SNR in linear units (Ivo, 2001),

$$\Delta\phi_{rms}^2 = \frac{1}{SNR_{in}}. \quad (2)$$

This translates into a maximum clutter suppression of,

$$CS = SNR, \quad (3)$$

where in this case the signal to noise ratio is in logarithmic (dB) units. Thus, if the system is very quiet and the clutter filters are sufficiently deep, the clutter rejection will be limited by the SNR. For example, suppose a system with a phase noise of only 0.06 deg (60 dB), has an SNR at the receiver of only 54 dB. The clutter rejection will be limited to 54 dB, though the rest of the system can support further rejection. This is an important result when evaluating clutter rejection at low signal levels, i.e. the signal

being evaluated must be well above the noise level. This is also important for receiver design, with overlapping channels to extend dynamic range. Depending upon the channel selected by logic, the clutter rejection may be limited in the overlap range.

The remainder of this paper will discuss how phase noise is quantified, primary contributors of phase noise in a radar system, develop the theoretical approximations to the phase noise from spectral measurements of the system and apply these measurements to estimate the maximum clutter suppression of the system. An experimental apparatus and techniques are described to evaluate the theoretical estimates. Finally, results from the DWSR-8501S/K system delivered to Evansville, Indiana for the United States National Weather Service is provided. In the end it is hoped that confusion between phase noise specifications, its assessment, and clutter rejection will be mitigated.

2. PHASE NOISE DESCRIPTORS

The phase noise of a device is described in many different ways. As we saw in the introduction, one

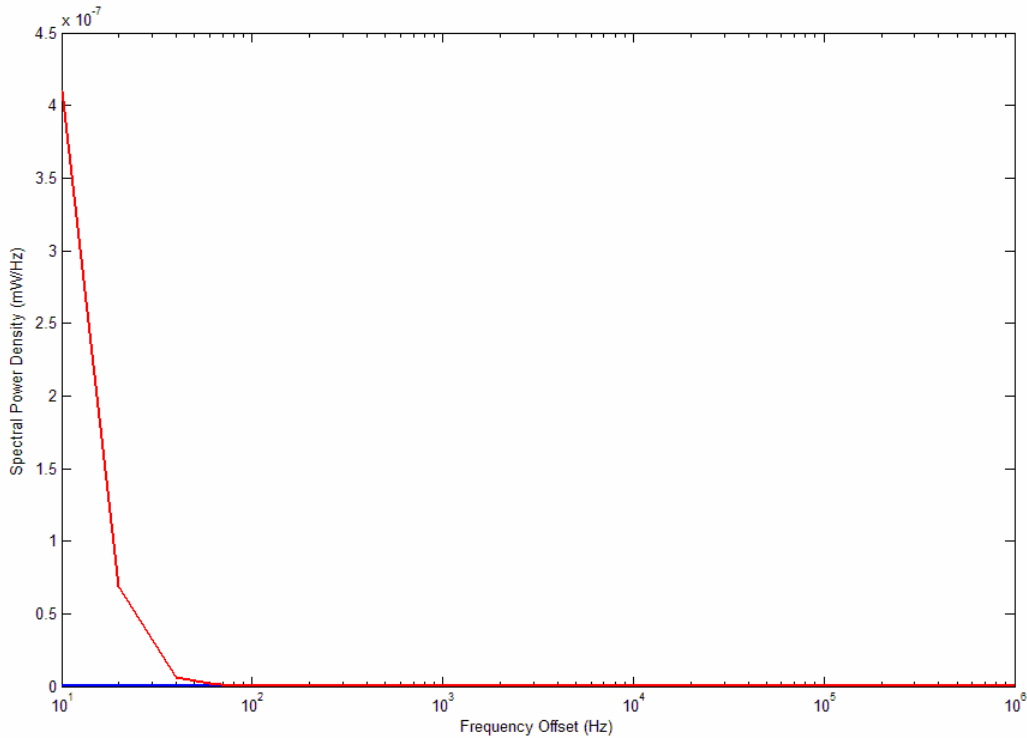


Figure 2. The phase noise spectrum of the DRS Oscillator in linear units, mW/Hz.

method is to specify the variance of the phase noise frequency distribution. This variance is typically termed in the amount of angle, such as 0.1 degree or in a coherency value in decibels such as 55 dB.

Another standard method is to list the signal strength (power) at the decade offset frequencies, 10 Hz, 100 Hz, etc. Table III is an example of such a description. This table is derived from measuring the phase noise spectral power at the listed offset frequencies, as shown in Figure 1. Though this is the standard practice, it is not performed uniformly. Some manufacturers list the power levels not at the specific decade frequency, but rather at the center of the decade. This curve is plotted in green in Figure 1. The values power spectral density values reported by the manufacturer are listed in the third column of Table III. As we can see, the spectral power in the center of the decade is much less than that at the actual frequency points. Thus, the same oscillator can appear to be much better depending upon representation.

Though the phase noise spectrum describes the phase noise of the system, it is not a straightforward measure of the system performance. In addition, the spectrum does not relate well to clutter suppression which, for radar, is of utmost importance.

Table III. Phase noise performance table.

Frequency Offset (Hz)	Spectral Power (dBc/Hz)	Spectral Power/Center (dBc/Hz)
10	-60	-72
100	-80	-85
1000	-84	-94
10000	-92	-94
100000	-102	-125
1000000	-128	-140

Thus, we need another measure that relates the two. One measure is the *integrated phase noise*. Integrated phase noise is just as it sounds, it is the integration of the phase noise spectrum. That is, by definition, to find the area under the spectral curve of the phase noise measurement.

The spectral plot is given in logarithmic units, i.e. dB/Hz. To find the area, this needs to be converted to linear units, i.e. W/Hz. Figure 2 shows the linear curve for the blue spectrum of Figure 1.

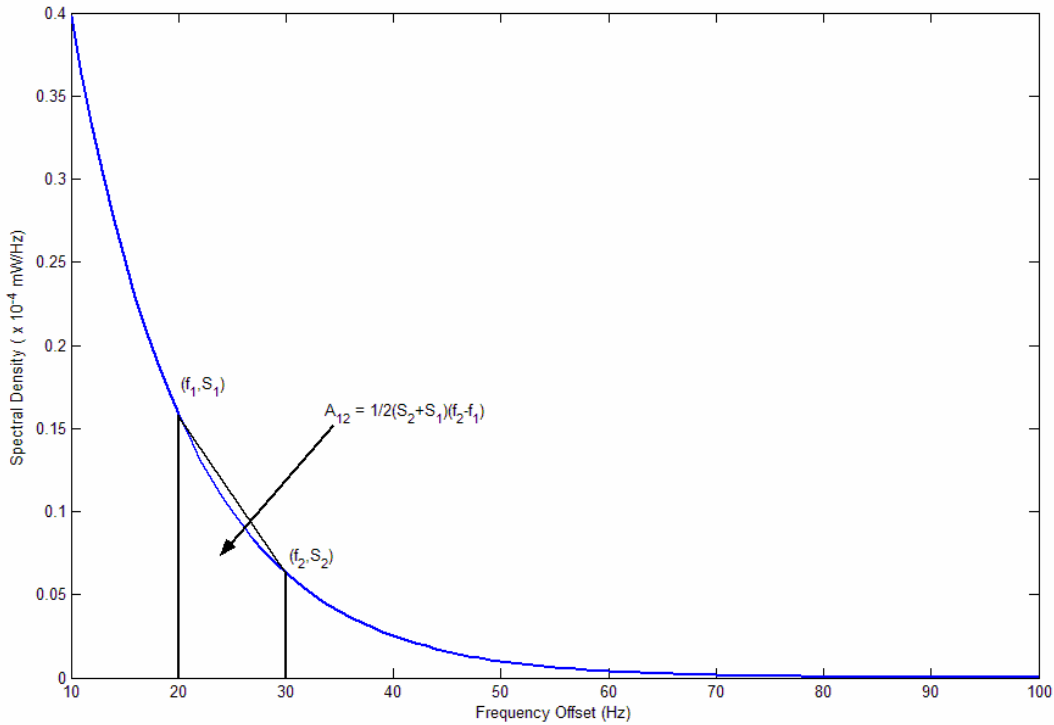


Figure 3 Finding the area under the curve between two points.

Now, to find the area, the frequency axis is divided into small segments. The spectral power density values for each side of a segment is used to estimate the area under the curve for that segment. This is shown in Figure 3.

The resultant area (represents the power between these two offset frequencies) is given by the formula,

$$P_n = \frac{1}{2} (S(f_{n-1}) + S(f_n)) (f_n - f_{n-1}). \quad (4)$$

All of the resultant areas are then summed to give the integrated phase noise, and the sum is converted to decibels.

Finding the area under the spectral curve (blue) of Figure 1, we find the integrated phase noise for this oscillator is -40 dBc.

3. PHASE NOISE MEASUREMENT

In the last section, we defined the descriptors of phase noise. We note that those descriptors are centered about the power spectrum of the signal. Thus, the measurement of phase noise is the measurement of this spectrum.

Phase noise measurement is as much art as it is science. The standard methodology for measuring the phase noise spectrum is to mix the signal from the device or system under test with that of a reference oscillator at the same frequency and view the spectrum of the results. Figure 4 schematically shows this method. To ensure an accurate measure of the device under evaluation, the phase noise of the reference oscillator should be significantly less than that of the device under test. Phase noise test equipment on the market implements this technique and outputs a spectrum of the device under test. A sample spectrum is shown in Figure 5.

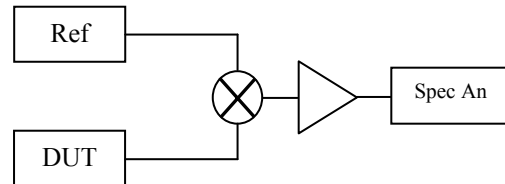


Figure 4. Schematic of a phase noise test configuration. The components identified as Ref is the reference oscillator, the DUT is the Device Under Test, and the Spec An is the spectrum Analyzer.

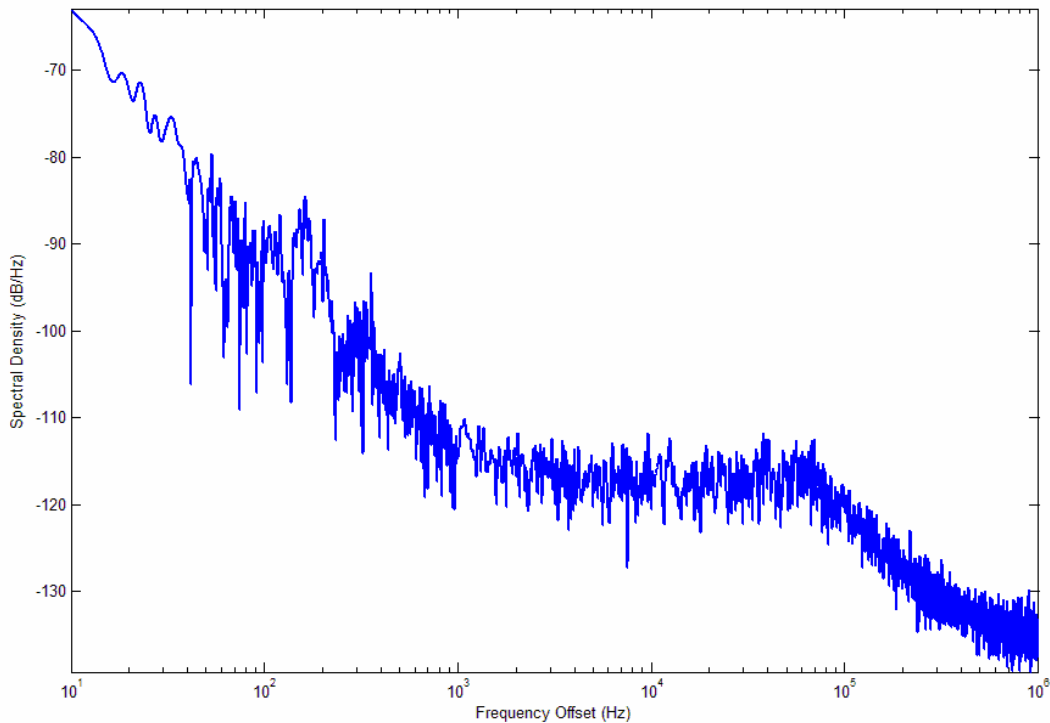


Figure 5. The spectrum of a device under test.

An alternative test arrangement is to split the signal from the device under test, and mix the result together, and obtain the spectrum. In this case, the resulting phase noise measurements will be twice as high (+3 dB higher) than the true phase noise of the system. This is due to the additive properties of signal mixing.

Throughout our studies, an Agilent E4445A Spectrum Analyzer with Phase Noise Personality function was used. This particular piece of equipment contains internal low noise sources with which to evaluate the phase noise. Figure 6 is a measured phase noise spectrum of a DRS Oscillator with the noise floor of the E4445A superimposed in blue. Note that the noise floor remains 10 to 20 dB below the oscillator spectrum. For each device for which data was collected, it was collected at least 10 times to allow statistics. We see that the phase noise of the measurement apparatus has minimal impact on the measurement of the oscillator phase noise.

Integrating the spectrum from the DRS oscillator shown in Figure 6, the integrated phase noise is found to be -54 dBc.

In radar, integrated phase noise is typically assessed via the clutter rejection measured with a delay line, a device that shifts the phase of the pulse by delaying it. The transmitted signal is fed into the delay line whose output is directed into the receiver channel for processing. The correlation between the delayed and transmitted signals is estimated. With weather radar, this method can be used as an objective assessment of clutter filter performance. However, as we will see, it is not a direct measure of integrated phase noise.

Before discussing the phase noise measurements, we look at some of the major contributors to system phase noise.

4. SYSTEM PHASE NOISE CONTRIBUTORS

Many components of a radar system can contribute significant amounts of phase noise. Timing jitter in the generation of triggers and pulses based upon those triggers will introduce phase noise. The characteristics of the high energy power supply and modulator, i.e. voltage/current variations inter- and intra- pulse, can greatly impact the phase noise characteristics of the system. Properties of the tube itself, i.e. whether it is a power oscillator (magnetron) or a power amplifier

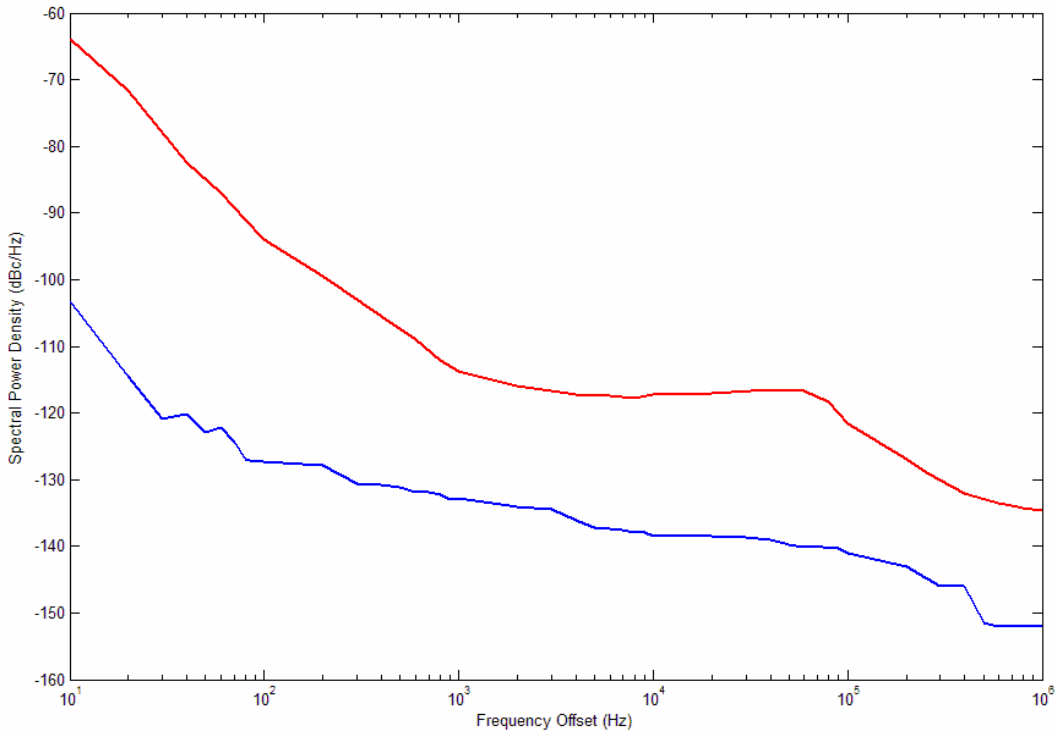


Figure 6. The phase noise spectrum of the DRS Oscillator in red with the noise floor of the E4445A superimposed in blue.

(klystron), will affect the phase noise of the system. If the tube is a klystron, variations in the magnetic field of the focus coils will affect the phase noise as well as the energy dispersion caused by the resonant cavities. The phase noise contributors in a complex system are themselves very complex. Minimizing the phase noise requires minimizing the noise from each and every contributor. In this section, we estimate the phase noise contribution from two of the primary contributors, the tube (magnetron or klystron) which includes the effects of the power supply and modulator, and the STABLE Local Oscillator (STALO).

Tube

The tube can be a significant contributor to the phase noise. Some tube types are better than others when it comes to phase noise. For example, the klystron, with an excellent power supply and modulator, can, in theory, achieve characteristic phase noise of 0.001 deg (Stone, 2004). Thus far, there are no power supply, modulator, and focus coil combinations that challenge a klystron tube phase noise characteristics. Hence, the phase noise

characteristics for klystron based systems are typically in the 0.1 - 0.2 deg range.

Magnetrons, through their normal operational modes, are much noisier. Typical magnetron phase noise values are on about 0.4 - 0.5 deg. However, recent studies have identified, empirically, techniques to improve the noise characteristics of magnetrons (Neculaes, 2003). These results are very promising; suggesting the possibility of magnetron based systems may one day approach the noise purity of klystrons.

Estimating the phase stability of the high power tubes encompasses estimating of the phase shift with respect to the transmitted frequency and the energy of the beam. For the high energy applications such as weather radar, the electrons are accelerated to relativistic speeds, thus this calculation requires the accounting of relativistic effects.

For example, in a high power klystrons, the electrons are accelerated to mildly relativistic speeds ($\sim 0.5c$ for the DWSR-8501S/K). Accounting for the relativistic effects, the resultant phase variation due to cathode voltage variation is given by, (Labbit, 2002),

$$\Delta\theta = \left\{ \frac{2\pi f D e}{m_0 c^3} \left[\left(\frac{eV}{m_0 c^2} + 1 \right)^2 - 1 \right]^{-3/2} \right\} \Delta V. \quad (5)$$

where f is the transmission frequency, D is the distance between the input and output cavities, V is the cathode voltage, ΔV is the rms ripple voltage on the cathode, e is the charge on the electron (1.6×10^{-19} C), c is the speed of light (3.0×10^8 m/s), and m_0 is the rest mass of the electron (9.1×10^{-31} kg).

For an S-band klystron ($f = 2700$ MHz) with a cathode pulse voltage of 60 kV, a 1 V ripple, and the distance between the input and output cavities of 0.559 m has a phase stability of approximately 0.0005 deg. This corresponds to a maximum clutter suppression of 66 dB.

As we will see, this relates very well with the empirical results obtained from the DWSR-8501S/K. Similar results were obtained with the DWSR-2501C/K. The question to be answered: are these results due to the modulator ripple or the limits of the STALO?

STALO

The STABLE Local Oscillator (STALO) is a low power RF oscillator that generates a signal that is mixed with an IF signal and injected into the Klystron for amplification or mixed with the magnetron burst and injected into an stable IF oscillator called the COHERent Oscillator (COHO). Thus, its noise characteristics are directly related to the radar system noise performance.

STALO's are typically frequency doubled oscillators. A low noise oscillator at a lower frequency is produced. The resulting signal is doubled repeatedly until the desired RF frequency is attained. Each doubling of frequency raises the phase noise of the oscillator by 6 dB. Thus, for an S-band STALO based upon a 10 MHz oscillator, reaching the RF frequency will result in an approximate 50 dB increase of phase noise.

This section is not a dissertation upon oscillator design. Rather, we discuss briefly the impact of the different oscillator configurations, fixed or variable, upon the phase noise.

Fixed Frequency

Fixed frequency oscillators use a single low noise base oscillator and frequency doubling circuitry that is optimized and tuned specifically for the desired frequency. Due to this, a great deal of focus can be placed on reducing the phase noise. Thus, a fixed frequency STALO will give the best phase noise performance.

Tunable

Tunable oscillators use multiple frequency doubling and halving circuitry to obtain the desired frequency in the desired steps. As noted before, the frequency doubling and halving operations all add phase noise to the oscillator. In addition, since the oscillator must operate over a range of frequencies, it is optimized for the frequency range.

Unfortunately, this also means that the phase noise cannot be minimized for any specific frequency. As such the phase noise is significantly higher. This can be mitigated by minimizing the number of intervals. The more frequency intervals (smaller tuning steps) an oscillator design contains, the higher the resultant phase noise.

5. RESULTS

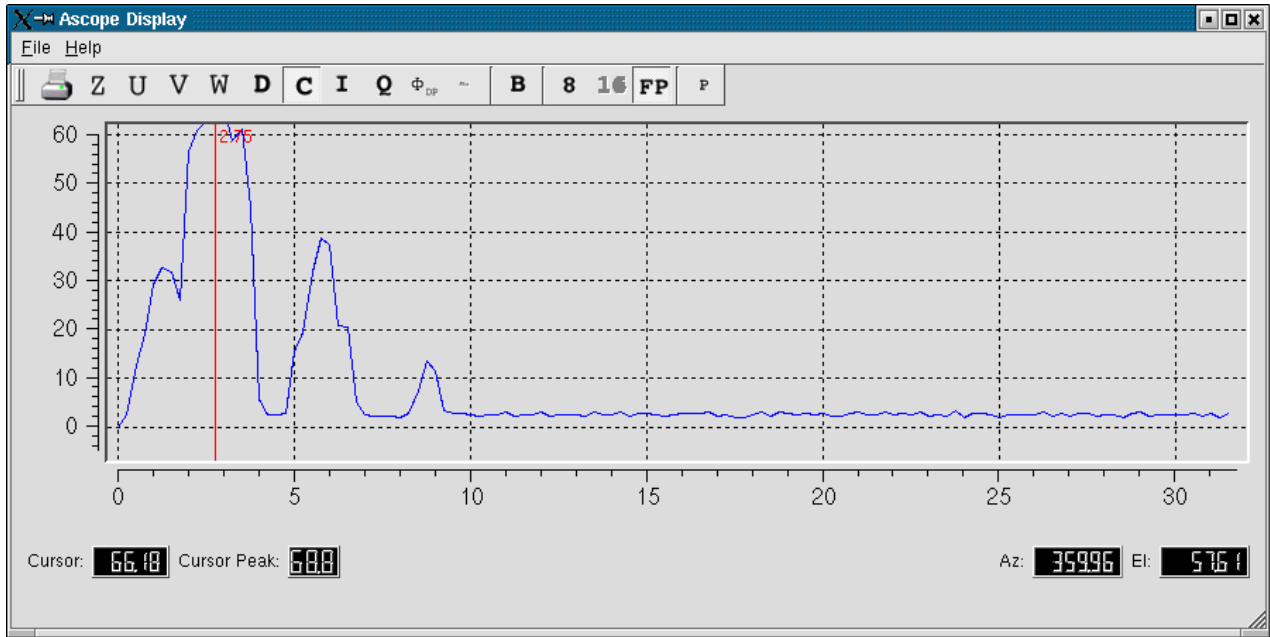
We evaluated the impact of the STALO phase noise on the clutter rejection of the radar system. This was done by characterizing the phase noise of the STALO using the Agilent E4445A Spectrum Analyzer Phase Noise Personality system. A Teledyne Brown 10 μ s SAW delay line was utilized to characterize the clutter rejection capability of the system. A 10 μ s delay line simulates clutter located a distance of 1.5 km ($cT_d/2$) from the radar. The clutter filters were applied to the received data and the resultant suppression noted. In addition, comparison with operational clutter rejection was obtained for some STALO's.

Figure 7 shows sample screen shots for the clutter rejection measurements from the DWSR-8501S/K delivered to Evansville, Indiana for the U.S. National Weather Service. Figure 7a shows that for the 10 μ s delay, the clutter rejection was about 66 dB. Figure 7b was obtained during the operation of the radar system. A clutter target was located approximately 21 km from the radar and the clutter rejection was measured. As we can see, for a clutter target located 21 km away, the rejection was still over 60 dB.

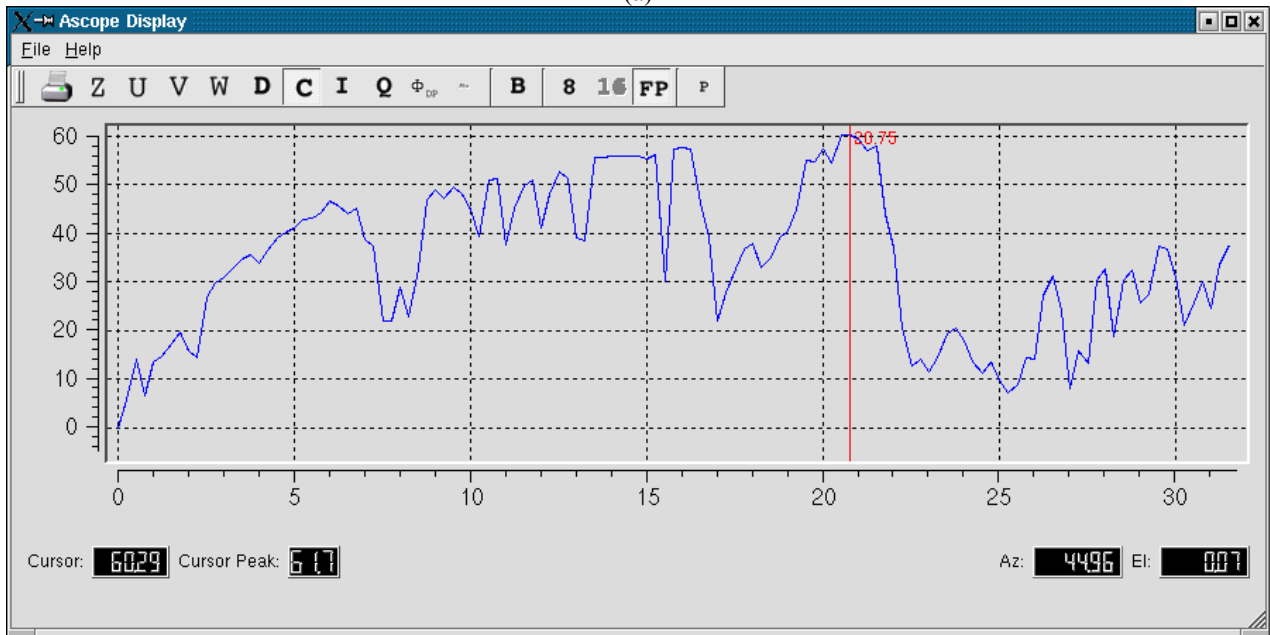
Four oscillators, listed in Table IV, were characterized in terms of clutter suppression and integrated phase noise. Their phase noise spectra are plotted in Figure 8.

Table IV. Clutter suppression as measured with a 10 μ s delay line and integrated phase noise for various synthesizers

STALO	Clutter Suppression (dB)	Integrated Phase Noise (dBc)
WSR-88D	65	-29
OSC - 1	52	-54
OSC - 2	38	-40
DRS Oscillator	66	-54



(a)



(b)

Figure 7. A-scope screen shots of the clutter rejection tests of the DWSR-8501S/K delivered to Evansville, Indiana for the United States National Weather Service, with the fixed frequency STALO installed. (a) A $10 \mu\text{s}$ RF delay line test, and (b) real clutter target approximately 21 km from the radar.

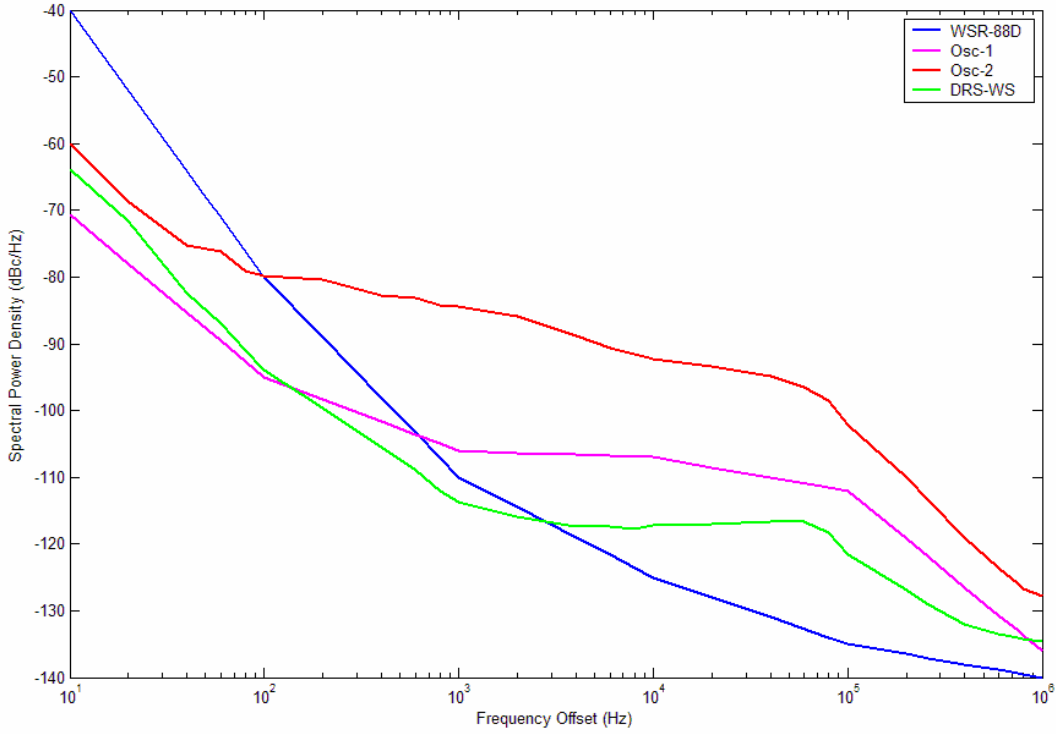


Figure 8. The phase noise spectra for the oscillators listed in Table IV. The WSR-88D legacy oscillator is in blue, Oscillators 1 and 2 are magenta and red respectively, and the DRS oscillator delivered with the Evansville DWSR-8501S/K is in green.

As we can see, the integrated phase noise does not correlate well at all with the clutter rejection. In fact the phase noise from small offset frequencies is clearly not as important as the noise from higher frequencies. This is a surprising result.

To explain the results summarized in Table IV, we need to look at the effect of a finite delay on the signal phase noise.

6. PHASE NOISE MODEL WITH DELAY

In developing the phase noise model with delay corrections, we need to understand the spectral function describing the signal before the addition of noise. Then, we can see what the addition of noise does to the signal and hence its behavior.

A very pure sinusoidal signal is described by,

$$s(t) = A_0 \sin(\omega_0 t + \phi_0) \quad (6)$$

where A_0 is the amplitude, ω_0 is the central frequency, and ϕ_0 is the initial phase. Transforming the signal from temporal space (time based) to frequency space through a Fourier transform,

$$S(\omega) = F(s(t)) = \frac{1}{\sqrt{2\pi}} \int_{-\infty}^{\infty} s(t) e^{j\omega t} dt, \quad (7)$$

the result is a delta function,

$$S(\omega) = \frac{A_0}{\sqrt{2\pi}} \delta(\omega - \omega_0). \quad (8)$$

The delta function has the properties of having value 1 at the center frequency and zero elsewhere, i.e.

$$\delta(\omega - \omega_0) = \begin{cases} 1 & \omega = \omega_0 \\ 0 & \omega \neq \omega_0 \end{cases}. \quad (9)$$

Thus, the spectral function for the pure sinusoidal signal described in Eqn (15) is,

$$S(\omega) = \begin{cases} \frac{A_0}{\sqrt{2\pi}} & \omega = \omega_0 \\ 0 & \omega \neq \omega_0 \end{cases}. \quad (10)$$

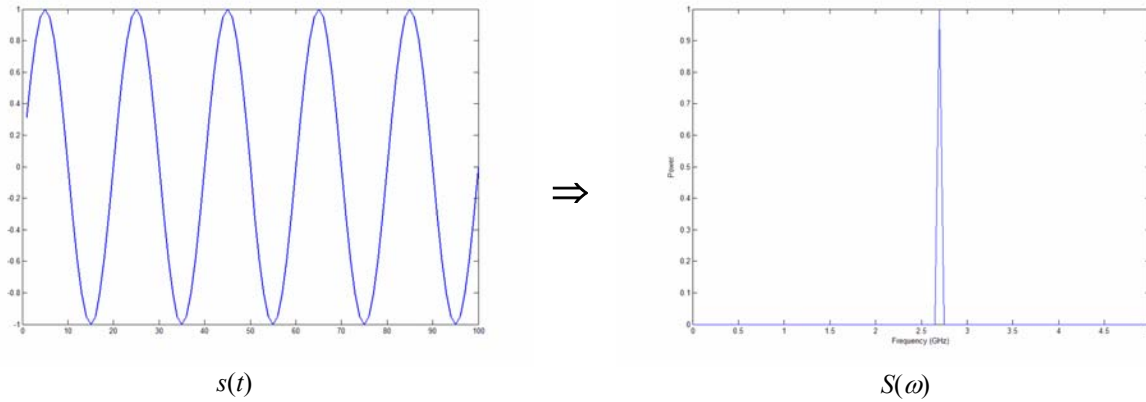


Figure 8. The spectral density (on the right) obtained via Fourier Transform of the signal on the left.

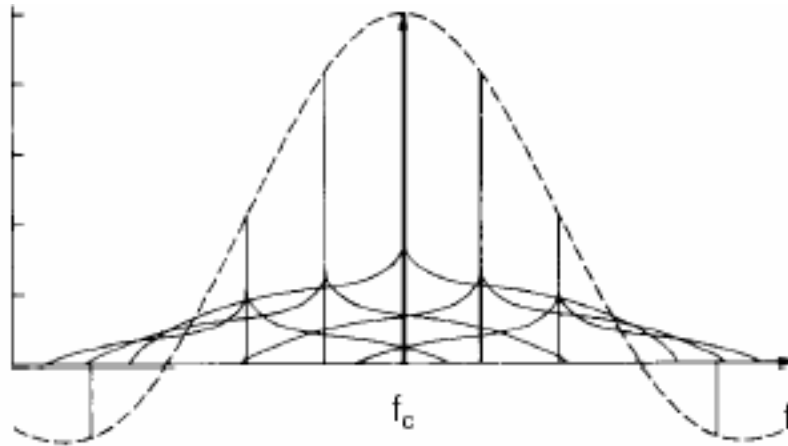


Figure 9. The effect of the phase noise across several PRT intervals. The vertical lines represent the pulses at the PRT interval. The dashed line is the power envelope in frequency space. The solid lines are the noise envelope.

The spectrum and related signal is summarized Figure 8.

Real signals do not present themselves as delta functions in frequency space. This is due to the stochastic processes associated with random noise. We can model the noise as normally stochastic function.

A mathematical model for the sinusoidal signal including the functions modeling the noise is (Scheer, 1993 and Goldman, 1989),

$$s(t) = [A_0 + \Delta A(t)] \sin[(\omega_0 t + \phi_0) + \Delta \phi(t)], \quad (11)$$

where the perturbation $\Delta A(t)$ is called the amplitude noise and $\Delta \phi(t)$ is the phase noise. The amplitude noise term is typically 20 dB or more less than the

phase noise. Thus, when measuring and estimating the noise contribution to signal degradation, the noise considered is phase noise. However, this assumption is not always true, particularly when relativistic effects are considered in high power systems.

Most weather radars transmit pulses at a constant rate or interval called the pulse repetition frequency PRF and pulse repetition time PRT respectively. In this case, we will have a number of overlapping phase noise curves in each PRT. The phase noise spectrum from one pulse enters the subsequent PRT's to increase its noise level. This effect is demonstrated in Figure 9.

Attempting to estimate all of the overlapping contributions within a PRT appears to be quite daunting, but appearances can be deceiving. If we look carefully at one of the PRT sections and consider

only the phase noise contributions from it and subsequent PRT intervals, it is clear that the integration of all the noise is in fact the same as integrating the signal in frequency space over the bandwidth,

$$I_{PN} = \int_{-f_{BW}}^{f_{BW}} S(f) df, \quad (12)$$

Functionally, we can integrate just one-half of the bandwidth and multiply the integral by two,

$$I_{PN} = 2 \int_0^{f_{BW}} S(f) df, \quad (13)$$

This integral is the integrated phase noise.

As an example, consider the following spectral function,

$$S(f) = \begin{cases} \frac{10^{-4}}{f^3} & 0 \leq f < f_{BW}/4 \\ \frac{10^{-8}}{f^2} & f_{BW}/4 \leq f < f_{BW}/2 \\ \frac{10^{-12}}{f^1} & f_{BW}/2 \leq f < 3f_{BW}/4 \\ \frac{10^{-13}}{f^0} & 3f_{BW}/4 \leq f < f_{BW} \end{cases}, \quad (14)$$

The integrated phase noise is,

$$I_{PN} = 2 \left[\int_0^{f_{BW}/4} \frac{10^{-4}}{f^3} df + \int_{f_{BW}/4}^{f_{BW}/2} \frac{10^{-8}}{f^2} df + \int_{f_{BW}/2}^{3f_{BW}/4} \frac{10^{-12}}{f^1} df + \int_{3f_{BW}/4}^{f_{BW}} 10^{-13} df \right]. \quad (15)$$

Realizing the first integral returns an indefinite result, we start the initial frequency not from zero, but slightly offset by an amount ε . Thus, Eqn. (15) becomes,

$$I_{PN} = 2 \left[\int_{\varepsilon}^{f_{BW}/4} \frac{10^{-4}}{f^3} df + \int_{f_{BW}/4}^{f_{BW}/2} \frac{10^{-8}}{f^2} df + \int_{f_{BW}/2}^{3f_{BW}/4} \frac{10^{-12}}{f^1} df + \int_{3f_{BW}/4}^{f_{BW}} 10^{-13} df \right]. \quad (16)$$

Integrating this function we have,

$$I_{PN} = 10^{-4} \left[\frac{1}{\varepsilon^2} - \frac{16}{f_{BW}^2} \right] + 10^{-8} \left[\frac{4}{f_{BW}} \right] + 10^{-12} \left[2 \ln \left(\frac{3}{2} \right) \right] + 10^{-13} \left(\frac{f_{BW}}{2} \right). \quad (17)$$

Assuming that $\varepsilon = 10$ Hz and the bandwidth is, $f = 1$ MHz (10^6 Hz), the integrated phase noise is,

$$I_{PN} = 1.0 \times 10^{-6} \text{ W or } -60 \text{ dBc}. \quad (18)$$

This system would achieve 60 dB of clutter suppression provided the signal to noise ratio is large enough.

This procedure seems simple enough provided we know the functional form of the phase noise. That is precisely the problem. When we take a phase noise measurement, we don't obtain an arithmetic form of the phase noise; rather a graphical form of the phase noise function is presented. If we obtain a set of the data values either from the plot or directly from the measuring device we can perform numerical integration.

Recall that the integration process finds the area between the curve and the axis. This process can be approximated by finding the area under the curve between two data points. As knowing the functional form is required to get an exact area, we can approximate this area by drawing a line between two nearest data points and finding the area of the resulting trapezoid. The area of a trapezoid is given by,

$$A_{trap} = \frac{1}{2} (y_1 + y_2) (x_2 - x_1). \quad (19)$$

If the data samples are close enough together, this technique will provide a good estimate of the curve. The phase noise plots are somewhat complicated because the Spectral function is described in logarithmic units (dBc/Hz). These values must be converted to linear units (W/Hz) before integration.

Delay Correction

Clutter rejection involves transmitting a signal which is scattered off the clutter target located at a distance R (Scheer 1993, Goldman 1989). The scattered signal returns to the radar. The total travel time is given by,

$$T_{delay} = \frac{2R}{c}, \quad (20)$$

where c is the speed of light. Thus, the reference signal is compared to this time delayed signal. Part of the delayed signal remains correlated with the reference signal. The correlated sections will cancel an amount related to their correlation. If the delay is zero, there is no decorrelation and the signal will cancel completely either to the transmitter stability or the Signal to Noise ratio, whichever is less. If the delay is infinite (very long or a very low PRF), the two signals are completely decorrelated and the suppression will be equal to the integrated phase noise.

The maximum suppression is between these two limits. The issue is to quantify the correction due to the delay time.

To estimate the form of the correction, we ignore the amplitude noise and look solely at the phase noise. With this approximation,

$$s(t) = A_0 \sin[(\omega_0 t + \phi_0) + \Delta\phi(t)]. \quad (21)$$

The instantaneous phase is given by the argument of the sine function,

$$\theta(t) = \omega_0 t + \phi_0 + \Delta\phi(t). \quad (22)$$

The instantaneous frequency is the derivative of the instantaneous phase,

$$\omega(t) = \dot{\theta}(t) = \omega_0 + \Delta\dot{\phi}(t). \quad (23)$$

The last term, $\Delta\dot{\phi}(t)$, is the frequency modulation of the signal.

Without knowing the exact form of $\Delta\phi(t)$, it is difficult to estimate the correction. To obtain an estimate in closed form, consider a sinusoidal modulation function,

$$\Delta\phi(t) = \gamma \sin(\omega_m t), \quad (24)$$

where γ is the modulation index given by,

$$\gamma = \frac{\omega_d}{\omega_m}, \quad (25)$$

ω_m is the frequency offset from the carrier, and ω_d is the maximum deviation frequency $\left(\frac{\omega_{BW}}{2}\right)$. The instantaneous phase and frequency are thus,

$$\theta(t) = \omega_0 t + \phi_0 + \gamma \sin(\omega_m t). \quad (26)$$

and

$$\omega(t) = \omega_0 + \gamma \omega_m \cos(\omega_m t). \quad (27)$$

Consider the difference between the instantaneous frequency at time t and that delayed by an amount $t - \tau$. Mathematically, this is written,

$$\Delta\omega(\tau) = \omega(t) - \omega(t - \tau). \quad (28)$$

Expanding the difference, we get,

$$\Delta\omega(\tau) = [\omega_0 + \gamma \omega_m \cos(\omega_m t)] - [\omega_0 + \gamma \omega_m \cos(\omega_m (t - \tau))], \quad (29)$$

and consolidating the terms, we have,

$$\Delta\omega(\tau) = \gamma \omega_m [\cos(\omega_m t) - \cos(\omega_m (t - \tau))]. \quad (30)$$

Using the trigonometric identity,

$$\cos(a - b) = \cos(a)\cos(b) + \sin(a)\sin(b), \quad (31)$$

we have,

$$\Delta\omega(\tau) = \gamma \omega_m [\cos(\omega_m t) - \cos(\omega_m t)\cos(\omega_m \tau) - \sin(\omega_m t)\sin(\omega_m \tau)]. \quad (32)$$

Simplifying we have,

$$\Delta\omega(\tau) = \gamma \omega_m [\cos(\omega_m t)[1 - \cos(\omega_m \tau)] - \sin(\omega_m t)\sin(\omega_m \tau)]. \quad (33)$$

To reduce Eqn. 33, consider,

$$\Psi = A \cos(a + b). \quad (34)$$

Using the trigonometric identity,

$$\cos(a + b) = \cos(a)\cos(b) - \sin(a)\sin(b), \quad (35)$$

to expand Ψ , we have,

$$\Psi = A[\cos(a)\cos(b) - \sin(a)\sin(b)]. \quad (36)$$

Defining $a = \omega_m t$ and comparing Eqn. 33 with Eqn. 36, we have,

$$\Delta\omega(\tau) = \Psi = A \cos(\omega_m t + b), \quad (37)$$

where,

$$A \cos(b) = \omega_m \gamma [1 - \cos(\omega_m \tau)] \quad (38)$$

and

$$A \sin(b) = \omega_m \gamma \sin(\omega_m \tau). \quad (39)$$

Squaring both of these terms and adding, we have,

$$A^2 = \omega_m^2 \gamma^2 \{ [1 - \cos(\omega_m \tau)]^2 + \sin^2(\omega_m \tau) \}. \quad (40)$$

Simplifying, we get,

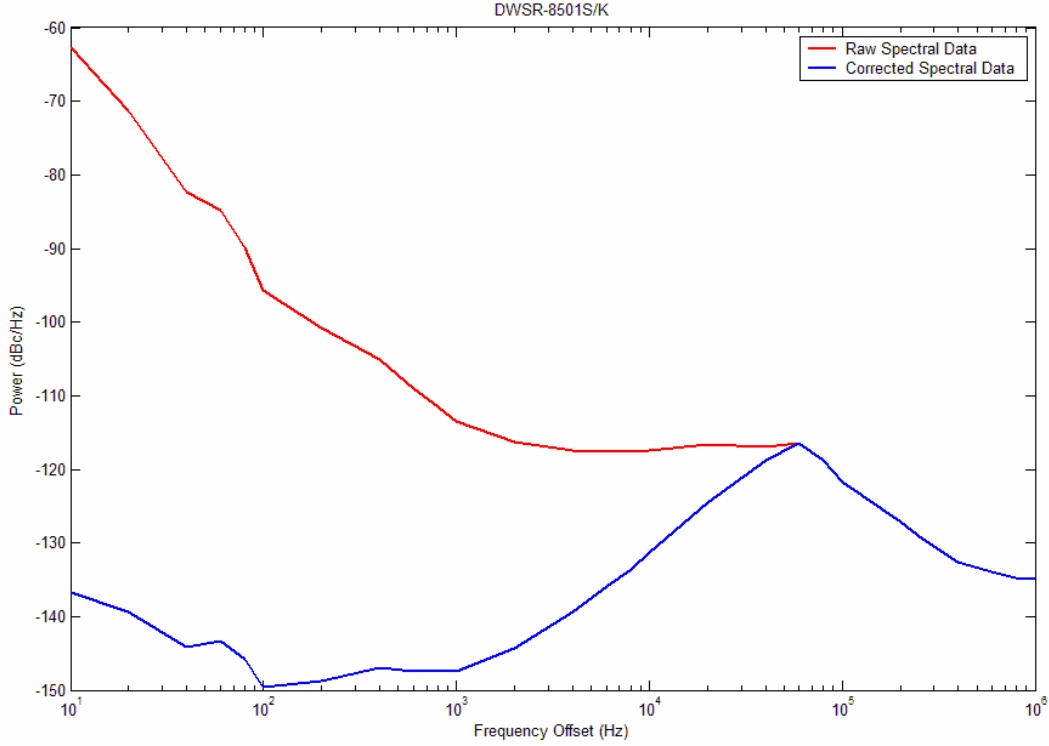


Figure 10. The impact of the delay correction on the phase noise spectrum. The red line is the measured phase noise. The blue line is the phase noise spectrum after the application of the delay correction.

$$A^2 = 2\omega_m^2 \gamma^2 [1 - \cos(\omega_m \tau)]. \quad (41)$$

Thus the instantaneous frequency deviation between the signal and a delayed version of the signal is,

$$\Delta\omega(t, \tau) = \omega_m \gamma \sqrt{2[1 - \cos(\omega_m \tau)]} \cos(\omega_m t + b). \quad (42)$$

Integrating this give us the instantaneous phase deviation,

$$\Delta\phi(t, \tau) = \gamma \sqrt{2[1 - \cos(\omega_m \tau)]} \sin(\omega_m t + b). \quad (43)$$

Essentially, Eqn. 43 states that a signal mixed with a delayed version of itself has its modulation index, γ , modified by a function dependent on the delay. It is this delay function that will provide the delay correction to the spectral function. The delay correction function to the spectrum will be,

$$\Gamma(\omega_m, \tau) = 10 \log[2\{1 - \cos(\omega_m \tau)\}]. \quad (44)$$

The correction will be valid up to an offset frequency, ω_m , that maximizes $1 - \cos(\omega_m \tau)$. This frequency, called the break frequency, will be when $\omega_m \tau = \pi$ or $\omega_m = \frac{\pi}{\tau}$. By definition, $\omega = 2\pi f$, so the break frequency in Hz is,

$$f_b = \frac{1}{2\tau}. \quad (45)$$

Figure 10 shows the effect of applying the correction to the phase noise spectrum. The solid red line is the measured phase noise spectrum. The blue line is the phase noise spectrum with the delay correction applied. As we can clearly see, the impact of low frequency offsets is dramatically reduced.

Table V summarizes the results of the correction applied to the oscillators listed in Table IV. Figure 11 is the corresponding corrected spectrum plots.

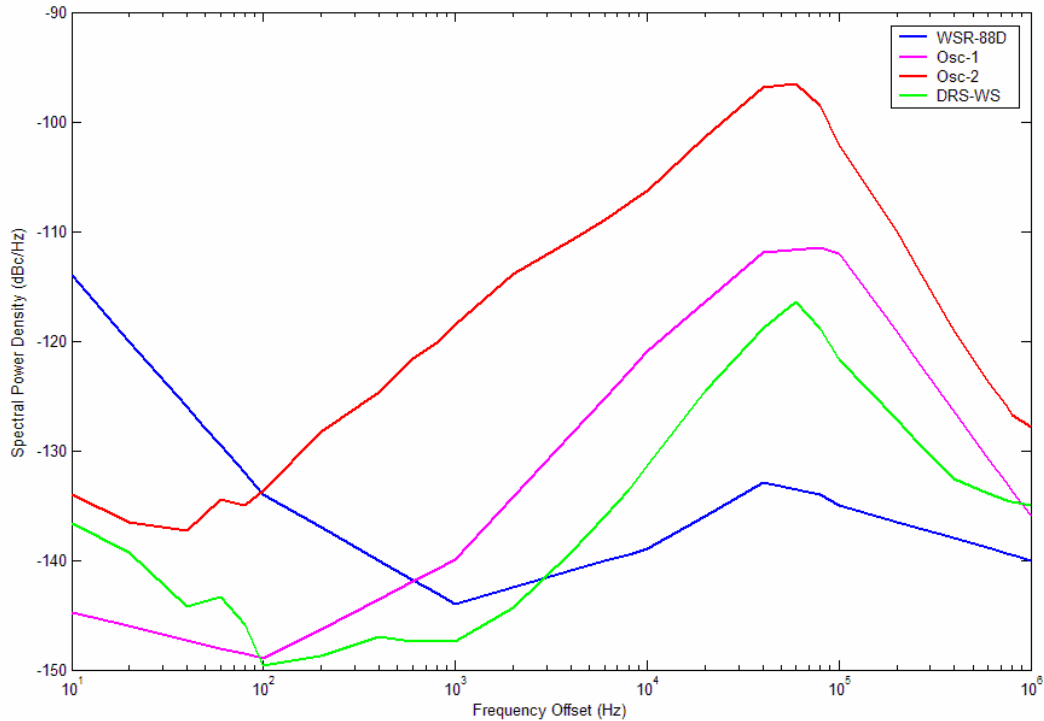


Figure 11. The corrected phase noise spectra for the oscillators listed in Table V. The WSR-88D legacy oscillator is in blue, Oscillators 1 and 2 are magenta and red respectively, and the DRS oscillator delivered with the Evansville DWSR-8501S/K is in green.

Table V. Clutter suppression as measured with a 10 μ s delay line and integrated phase noise for various synthesizers. Delay correction applied to the data.

STALO	Clutter Suppression (dB)	Integrated Phase Noise (dBc)	Integrated Phase Noise w/ Correction (dBc)
WSR-88D	65	-29	-75
OSC - 1	52	-54	-57
OSC - 2	38	-40	-45
DRS Oscillator	66	-54	-74

Once the correction is applied, it is clear that the phase noise performance at high offset frequencies is of much greater interest for clutter rejection than those at low frequency. In addition, from the integrated phase noise, we find that the WSR-88D legacy oscillator as well as the DRS oscillator can easily support the measured performance.

A result of this analysis is that as the clutter appears farther out in range (longer delay time), the ability of the system to cancel it is significantly degraded. This also is important for evaluating the specifications of a weather radar system.

7. CONCLUSION

In this paper, we looked at the relationship between system phase noise and clutter rejection. We noted that the major contributors to a system's phase noise is the power supply, modulator, and tube combination and the STALO. We used STALO's with different phase noise characteristics, transmitted pulses through a 10 μ s delay line (corresponding to clutter located a mere 1.5 km from the radar, and determined the resulting clutter suppression.

From the data and analysis we are able to conclude that the relationship between system phase noise and clutter rejection is very complicated. First and foremost there needs to be sufficient signal with respect to noise for maximum clutter rejection. The

signal to noise ratio (SNR) provides a limit to the amount of clutter rejection available.

Provided the SNR is great enough, the maximum clutter rejection is related to the integrated phase noise *corrected for the delay*. The net result, for STALO design is that the phase noise spectral power density levels near the carrier frequency are not as important for clutter rejection as those at greater frequency offsets from the carrier. Thus in designing a low noise STALO, more effort should be expended at reducing high frequency noise.

8. REFERENCES

Einstein, A., 1905: Does the inertia of a body depend upon its energy content?, *Annalen der Physik*. **18**:639.

Goldman, S., 1989: Phase Noise Analysis in Radar Systems, John Wiley and Sons, 518.pp.

Ivo, V. and H. Josef, 2001: Phase Noise Measurement, *Proceedings of the Radioelectronika 2001, BRNO 2001*, pp. 131 - 134.

Labbit, Melvin, 2002: Personal Communication, MIT Lincoln Laboratory.

Neculaes, V.B., R. M. Gilgenbach, Y.Y. Lau, 2003: Low Noise Microwave Magnetrons by Azimuthally Varying Axial Magnetic Field, *Applied Physics Letters*, **83**:10, pp. 1938 - 1940.

Scheer, J. and J. Kurtz, 1993: Coherent Radar Performance Estimation, Artech House, pp.446.

Stone, Melvin, 2004: Personal Communication, MIT Lincoln Laboratory.